SUPPLEMENTARY MATERIAL FOR

PHENOLOGICAL PLASTICITY WILL NOT HELP ALL SPECIES ADAPT TO CLIMATE CHANGE

Anne Duputié[1,2*], Alexis Rutschmann[2,3,*], Ophélie Ronce[4], Isabelle Chuine[2]

CONTENTS

[1] Laboratoire Génétique et Evolution des Populations Végétales, CNRS UMR 8198, Université Lille1, F-59655 Villeneuve d'Ascq cedex, France.

[2] CEFE UMR 5175, CNRS - Université de Montpellier - Université Paul-Valéry Montpellier - EPHE – 1919 route de Mende, 34293 Montpellier cedex 05, France.

[3] Station d'Ecologie Expérimentale du CNRS à Moulis, Unité de Service et Recherche 2936, Moulis, 09200 Saint-Girons, France.

[4] Institut des Sciences de l'Evolution Université Montpellier 2, CNRS, IRD, CC65, Place Eugène Bataillon, 34095 Montpellier cedex 5, France.

I. THE MODEL PHENOFIT

This model was introduced by Chuine & Beaubien (2001). The version of the model used in the present analysis is presented in the Supplementary Information file to the paper by Gritti *et al.* (2013). For clarity, we here reproduce most of the relevant explanatory text.

The model PHENOFIT relies on the assumption that species adaptation to abiotic conditions is tightly related to its capacity to synchronize its annual life cycle with seasonal climatic variations directly impacting its survival and reproductive success. It simulates the precise phenology and levels of resistance to drought and cold stress of an average individual of a tree species given local climatic conditions to yield a reproductive success and a survival probability. The product of survival and reproductive success is used as a proxy for fitness, and for the probability of occurrence. This model does not make use the observed distribution of the species to produce its output. Note that this model does not rely on observed species distribution.

1. DESCRIPTION OF THE VERSION OF THE MODEL USED IN THIS STUDY

(1) PHENOLOGY

Leaf unfolding and flowering dates are determined by daily temperatures using the sequential model first described by Sarvas (1974), and assuming first an endodormancy phase, followed by an ecodormancy phase. During endormancy, bud development is halted completely – this dormancy is broken after a cold period. During the ecodormancy phase, bud development can take place provided weather conditions are favourable – this dormancy is broken after a warm period. Leaf unfolding takes place once both phases have ended. Chilling units accumulation (allowing to break endodormancy) was modeled using a function defined by Wang & Engel (1998) for *Quercus petraea,* the function presented in Chuine (2000; eqn 8) for *Fagus sylvatica,* and the triangular function of Kramer (1994) for *Pinus sylvestris.* Forcing unit accumulation (allowing ecodormancy break) was defined by a sigmoid function for all three species. In these models, leaf unfolding and flowering dates depend on winter and spring temperatures only.

Fruit maturation date is calculated following Chuine & Beaubien (2001) for the deciduous species, and following a degree-day sum for *Pinus sylvestris* (Cheaib *et al.* 2012).

For leaf senescence, we used the model of Delpierre *et al*. (2009) for *Fagus sylvatica* and *Quercus petraea*. Leaf senescence dates thus depend on temperatures and on photoperiod.

(2) REPRODUCTIVE SUCCESS

The reproductive output corresponds to the proportion of mature fruits by the end of the year.

It is calculated as the product of fruit maturation success and the proportion of fruits that reach maturation (i.e. have not been killed by frost all along the season since the flower primordia). The proportion of fruits that reach maturity is calculated following the frost damage model of Leinonen (1996) parameterized for flowers and fruits. The success of maturation depends upon the proportion of uninjured leaves available for photosynthesis following a sigmoid function with parameter *pfe50*, the proportion of injured leaves that reduces by 50% the flux of photosynthetic assimilates going to the fruits. It also depends on a drought index calculated with a water balance using precipitation, actual evapotranspiration and soil water holding capacity. Finally, it depends on temperature

which determines the course of maturation. Fruits maturation date follows a normal distribution within the tree crown, defined by $E_c \sim \mathcal{N}(matmoy, sigma)$, with *matmoy* and *sigma* expressed as a sum of developmental units and *sigma* chosen so that 95% of the fruits mature within one month (Chuine & Beaubien 2001).

(3) SURVIVAL TO STRESSES

Two kinds of stress are considered: frost and drought.

A lethal frost temperature is used in the model but never plays a role in determining species range limits.

Frost injury on buds, leaves, flowers and fruits is modeled according to the model of Leinonen (1996). Frost hardiness depends upon the organs' developmental stage, photoperiod and temperature. Frost hardiness is highest during the dormancy phase, and lowest during bud burst. Frost can injure buds, leaves, flowers and fruits.

In this version of PHENOFIT, survival to drought or flooding was implemented as follows: four limits of yearly precipitation were set; outside the outer precipitation limits, survival was assumed to be 0.1; inside the inner limits, it was assumed to be 1 and it varied linearly between the inner and outer limits.

(4) INPUT AND OUTPUT VARIABLES

In the version of PHENOFIT used in this study, input variables are daily minimal and maximal temperatures, and monthly amount of precipitation. The model outputs a proxy for fitness within [0,1], which is the product of survival and reproductive success, for each cell and each year. For each cell, fitness is averaged over a 20-year time period (1981-200 for the "current" climate; 2081-2100 for scenarios) to produce the maps.

2. MODEL PARAMETERIZATION

(1) PHENOLOGY

The model parameters are found through minimizing the residual sum of squares using the simulated annealing algorithm of Metropolis following Chuine et al. (1998), as implemented in the software PMP (Chuine *et al.* 2013).

The fitting procedure uses observations of leaf unfolding, flowering, fruit maturation and leaf senescence dates, in different populations of the same species, together with daily climatic observations.

Fagus sylvatica: For *Fagus sylvatica,* we used observations from the French phenological database (Observatoire des Saisons, GDR2968[5]), field observations by Vitasse (2009) in the Pyrenees, and observations from the European phenological database[6].
Only sites within 20 km and 200 m altitude of a weather station providing a complete record of daily temperatures spanning from the autumn preceding the observation to the end of the year of observations were retained. Daily weather data from the closest meteorological station were obtained from MeteoFrance[7] for French sites, and from the National Climatic Data Center (NCDC[8]) for sites outside France.
Only observations posterior to 1972 were considered, and sites with fewer than 10 observations in total were removed. Because observations of leaf unfolding and leaf senescence were numerous and spatially biased, we randomly selected a maximum of 50 observations per event per 5°x5° cell. This selection procedure resulted into the use of 575 observations for leaf unfolding (the remaining 2610 observations were only used to validate the phenological model) and 560 for leaf senescence (the remaining 1674 observations were used for model validation only). Flowering was less documented, with only 23 observations (all of them used to calibrate the flowering model). Fructification is poorly documented for this species, with highly variable dates reported for very close stations on any given year. Probably for this reason, we were unable to fit a fructification model with reasonable predictive power using all available observations. We thus only used observations performed by a single investigator (F. Bonne, INRA Nancy), in Northeastern France (23 observations).

Quercus petraea: The phenology of *Quercus petraea* is not documented in the European phenological database; hence we only used phenological observations retrieved from the French database and from Vitasse (2009). Leaf unfolding and leaf senescence observations encompassed the period 1997-2011; flowering dates were observed in 2006-2008; and fruit maturation from 1990 onwards.
In total, we used 522 leaf unfolding observations, 296 fructification observations, and 228 observations for leaf senescence. Because recent observations of flowering were unavailable, the flowering model was calibrated using the delay between leaf unfolding and flowering, from 202 more ancient phenological observations (1900-1963) from the French phenological database. Daily weather data from the closest meteorological station (within 20 km and within 200 m altitude) were obtained from MeteoFrance.

Pinus sylvestris: Available phenological observations were scarce, resulting in doubtful parameter values. We therefore used the model parameters obtained by Kramer (1994) on a German provenance.

---

[5] http://www.gdr2968.cnrs.fr; all links in this document last visited on February 18th, 2015.
[6] http://www.pep725.eu/
[7] http://publitheque.meteo.fr/okapi/accueil/okapiWebPubli/index.jsp
[8] http://www7.ncdc.noaa.gov/CDO/cdoselect.cmd?datasetabbv=GSOD

Note that even though phenological observations span a wide area, especially for *Fagus sylvatica*, a single parameter set was determined per species. In this study, thus, local adaptation is not taken into account.

The sites used for model parameterization are shown on the following maps:

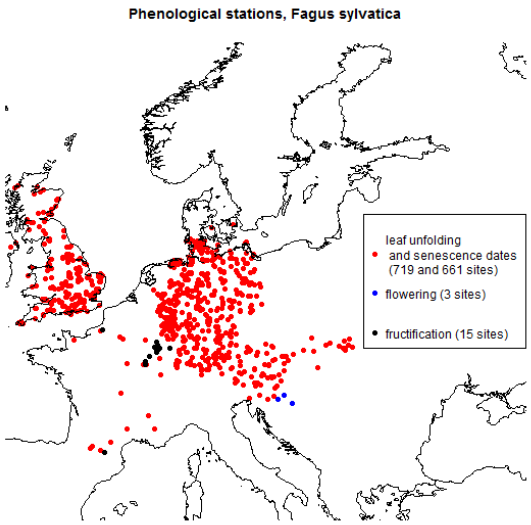

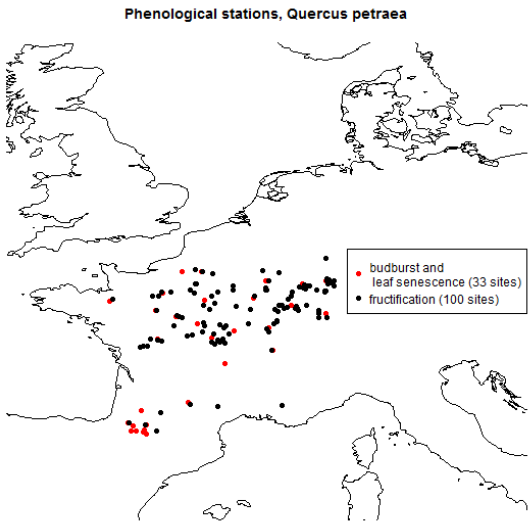

(2) SURVIVAL TO STRESSES

Precipitation limits determining the resistance to drought stress were taken from the French Forest Inventory[9].

Lethal temperatures were those identified by Sakai & Weiser (1973). Parameters for the frost damage model were those of Leinonen (Leinonen 1996), except the minimum and maximum hardiness, which were compiled from the literature (Morin *et al.* 2007; Charrier 2011).

[9] http://inventaire-forestier.ign.fr/spip

(3) MODEL PARAMETERS

Model parameters are provided in Tables S1 (*Fagus sylvatica* and *Quercus petraea*) and S2 (*Pinus sylvestris*).

Table S1. Parameters used in PHENOFIT (*Fagus sylvatica* and *Quercus petraea*). The number *n* of observations used to fit the leafing and fructification models is given, as well as the proportion of variance in bud burst/fructification dates explained by the model (R^2).

	Fagus sylvatica		***Quercus petraea***
Leaf unfolding date			
a	0.007	*Topt*	2.7
b	-0.347	*Tmin*	-48.0
c	-13.1	*Tmax*	30.2
d	-0.138		-0.4
e	17.3		9.0
*C**	194.0		157.7
*F**	8.2		22.5
n	*575*		*172*
R^2	*0.45*		*0.71*
Flowering date			
*F***	10.7		28.49
Fruit maturation date			
g	-0.2		-0.7
h	14.7		10.3
Fcrit	9.0		87.1
Top	5.0		5.0
matmoy	100.0		66.3
sigma	3.7		4.6
pfe50	0.6		0.6
n	*23*		*296*
R^2	*0.49*		*-0.07*
Leaf senescence date			
Pstart	13.4		11.3
Tb	30.0		22.2
x	1		2
y	2		0
Ycrit	570		1340
n	*560*		*228*
R^2	*0.19*		*0.24*

	Fagus sylvatica	***Quercus petraea***
Frost hardiness		
T1	10	10
T2	-16	-16
NL1	10	10
NL2	16	16
Fruit		
Frmax1	-6	-12
Frmax2	-20	-50
Leaf		
Flmin	-5	-8
Ftlmax	-8	-10
Fplmax	-12	-14
Flower		
Ffmin	-5	-7
Ftfmax	-8	-10
Fpfmax	-12	-14
Precipitation Limits		
PPminouter	450	460
PPmininner	490	490
PPmaxinner	1250	1250
PPmaxouter	1600	2000

Table S2. Parameters used in PHENOFIT (*Pinus sylvestris*). Parameters for the bud burst model were extracted from Kramer (1994).

Leaf unfolding date (from Kramer 1994)	
Ti	-13.8
Top	-1.2
Ta	16.5
b	-0.1
c	37.6
*C**	85.3
*F**	2.4
n	*369*
R²	*0.33*
Flowering date	
*F***	2.2
Fruit maturation date	
Tb	5.0
Fcrit	500.0
sigma	57.0
pfe50	0.6
Precipitation Limits	
PPminouter	430
PPmininner	480
PPmaxinner	1300
PPmaxouter	2100

Frost hardiness	
T1	10
T2	-16
NL1	10
NL2	16
Fruit	
Frmax1	-10
Frmax2	-50
Leaf	
Flmin	-5
Ftlmax	-47
Fplmax	-18.5
Flower	
Ffmin	-10
Ftfmax	-47
Fpfmax	-18.5

II. MODEL VALIDATION

1. REFERENCE DISTRIBUTION MAPS

For all three species, we compared the distribution of fitness, as modeled by Phenofit (using the empirical reaction norms for phenological events: "plastic" treatment), to the observed distribution of the species. The observed distribution was compiled from several sources of data: Atlas Flora Europaea AFE[10] (Jalas & Suominen 1972-1999; Lahti & Lampinen 1999), the EUFORGEN dataset[11], the Joint Research Center dataset[12], the map of the potential vegetation of Europe[13] (Bohn *et al.* 2004), and data from the Global Biodiversity Information Facility[14].

Distribution data obtained from these sources of data were either upscaled or downscaled to the resolution of 10'. AFE occurrence data (whether native or alien) were downscaled to 10', by attributing occurrences from one 50-km AFE cell to all 10' pixels overlapping this cell. The EUFORGEN dataset consists of continuous areas and punctual occurrences: occurrences were attributed to each pixel of the 10' grid overlapping a continuous area, or containing at least one punctual occurrence. The EuroVegMap dataset is provided as a series of polygons corresponding to potential vegetation types (including plantations) at a 2 km spatial scale. Whenever a focal species is known to occur, it appears as present over the whole polygon. For each species, 10' pixels were attributed the value "occurrence" if they were overlapping totally or partly a polygon containing the species. JRC data record species abundances within forests, at 1 km resolution (these data are based on extrapolations of forest inventory data). JRC data were transformed into presence-absence data through attributing an "occurrence" record to each 10' pixel overlapping at least one 1-km JRC pixel with positive abundance. Punctual occurrences referenced in GBIF data were attributed to the pixel overlapping the record. Occurrences were joined among sources, resulting in the occurrence maps presented on Figure S0 (top row).

[10] http://www.luomus.fi/en/atlas-florae-europaeae-afe-distribution-vascular-plants-europe
[11] http://www.euforgen.org/distribution-maps/
[12] http://forest.jrc.ec.europa.eu/
[13] http://www.floraweb.de/vegetation/dnld_eurovegmap.html
[14] http://www.gbif.org/

2. MODEL VALIDATION

The Area Under the Receiver Operating Curve (Swets 1988) of the spatial projections of fitness obtained with PHENOFIT, for the current period and the "plastic" treatment, were derived with respect to the consensual maps (Figure S0 below).

Using 0.1 as a threshold for fitness, above which the species is deemed as "present", resulted in accuracies of 81%, 83% and 69% for *Fagus sylvatica*, *Quercus petraea* and *Pinus sylvestris,* respectively.

Figure S1: Observed distribution (top row) and modelled fitness (bottom row) of the three species with treatment 0, under historic conditions. AUC values are shown for each species. Note that the observed distribution maps are derived from several data sources, which sometimes show large discrepancies, e.g. in the case of *Pinus sylvestris* in northern Europe (Duputié *et al.* 2014).

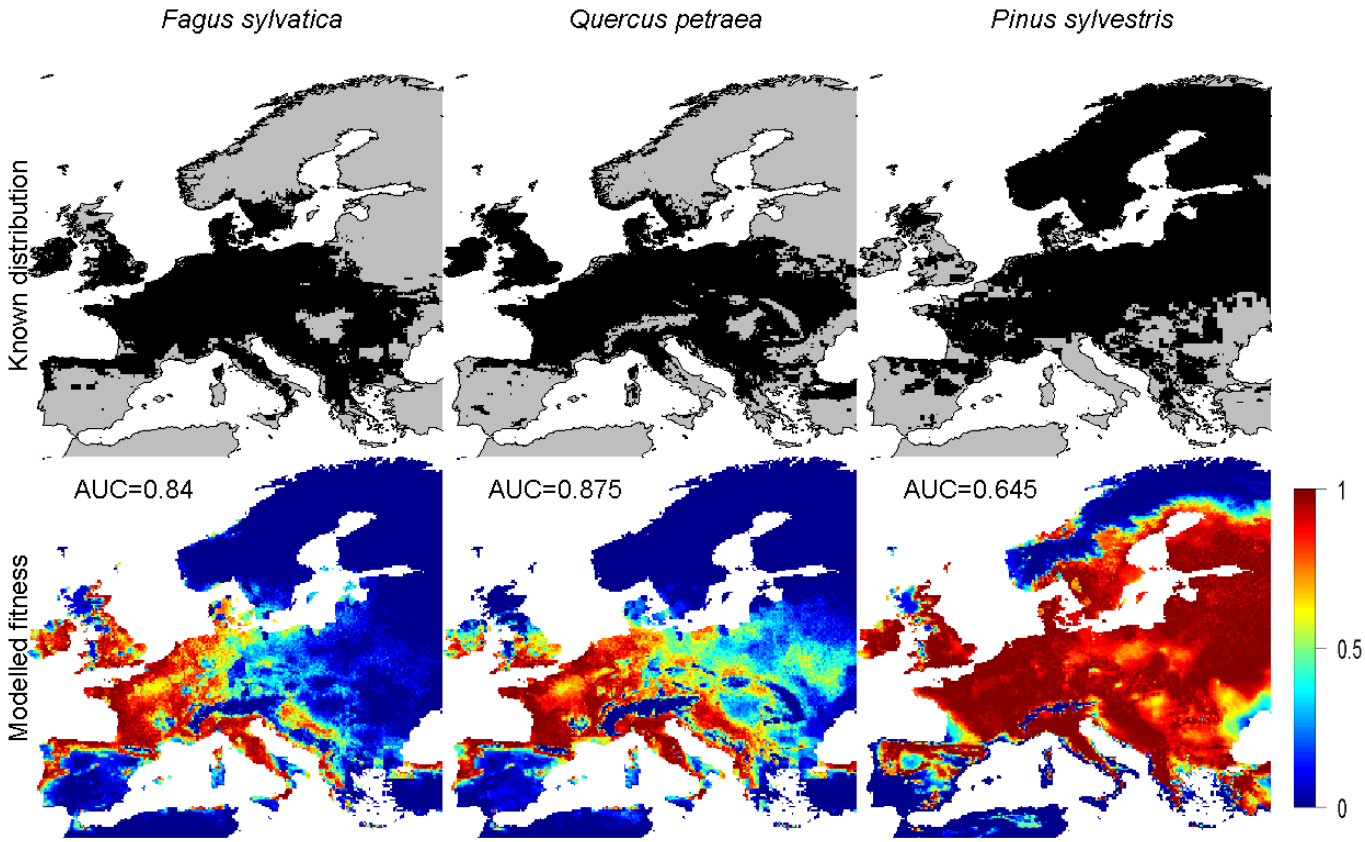

III. SUPPLEMENTARY FIGURES

1. FIGURE S2

Figure S2. Fitness distribution maps of treatments were compared on a pixel-by-pixel basis in the geographic and niche space. Figure S1a-d shows, as an example, maps of the realized distribution of *Quercus petraea* (a), of the modelled fitness of treatment 0 for this species under historical conditions (b); of the modelled fitness for treatment 2c for the same period (c), and of the difference between the two (treatment 0 – treatment 2c; d). Fig. S1d thus shows the total contribution of phenological plasticity to fitness. Regions where plasticity is adaptive appear in red; regions where the reaction norms of phenology to climate are non adaptive appear in blue.

Figures S1 e-h are projections of Figs S1 a-d in the climatic space, defined by a PCA on bioclimatic descriptors. The first (horizontal) axis is mostly carried by temperatures, with cold regions to the left and warm regions to the right. The second (vertical) axis is mostly carried by precipitations, with dry regions to the bottom and wet regions to the top.

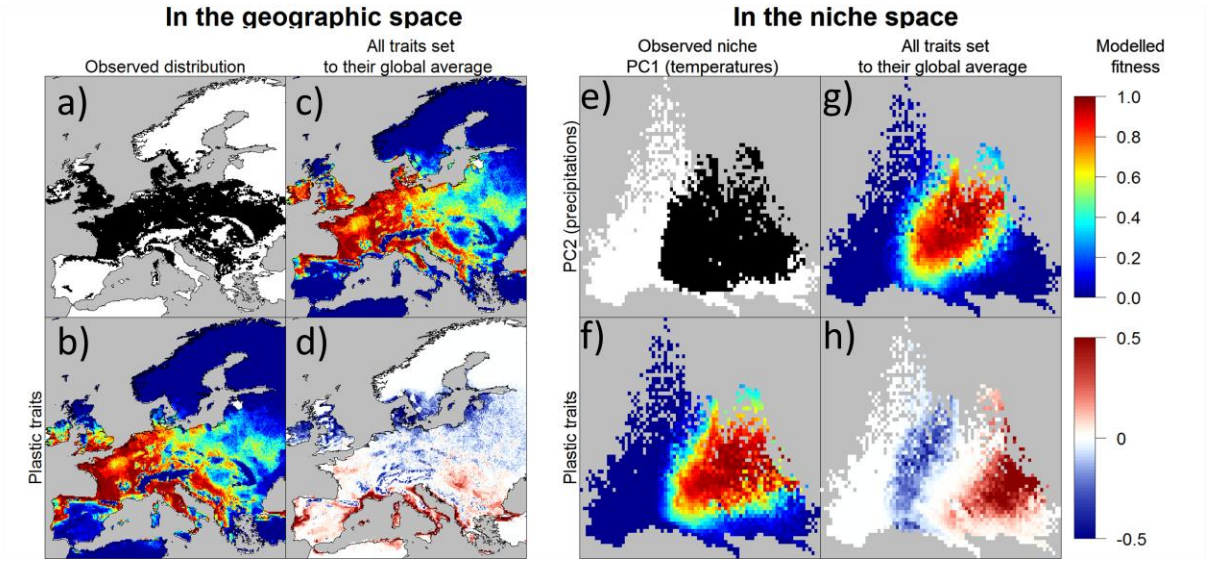

2. FIGURE S3

Figure S3. Density of geographic pixels in the climatic space of Europe under historical and future conditions under both scenarios (horizontal axis: PC1 related to temperatures, increasing towards the right; vertical axis: PC2 related to precipitation, increasing towards the top). Note the logarithmic scale for the number of geographic pixels. Under future conditions, the climatic space shifts and expands towards the right (higher temperatures) and top (higher precipitations), but regions with higher precipitations are very scarce.

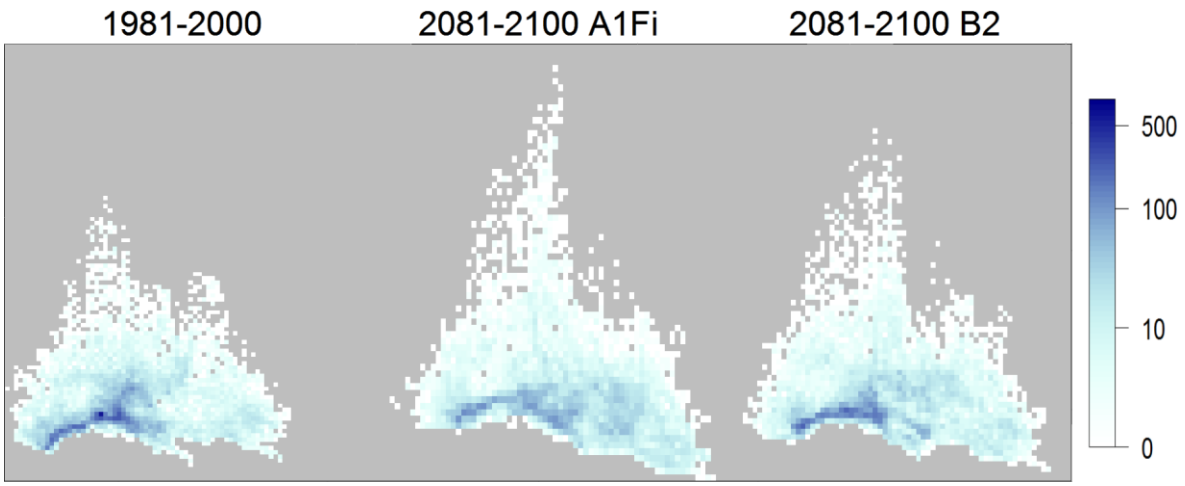

3. FIGURE S4

Figure S4. As main text Fig. 2 but showing results for manipulation of spring events only. This figure shows the total effect of plasticity of spring events (treatment 0 – treatment 2a for the historical period; treatment 0 – treatment 3a for scenario A1Fi), in the geographic (top rows) and climatic (bottom rows) spaces. For *Pinus sylvestris,* only spring events were manipulated, hence this map is as on Fig. 2.

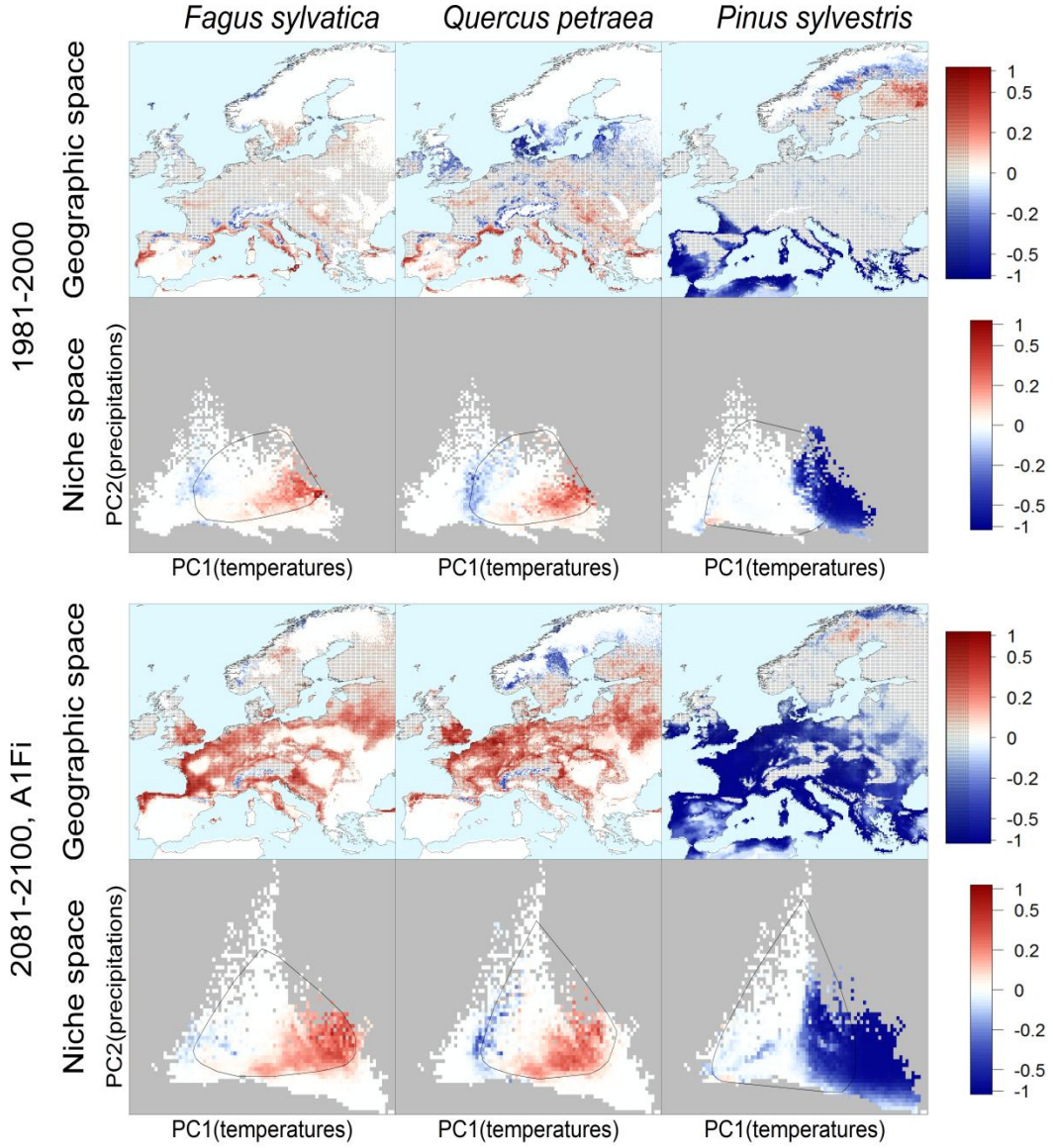

4. FIGURE S5

Figure S5. As main text Fig. 2 but showing results for manipulation of fall events only. This figure shows the total effect of plasticity of fall events (treatment 0 – treatment 2b for the historical period; treatment 0 – treatment 3b for scenario A1Fi), in the geographic (top rows) and climatic (bottom rows) spaces. Note that no fall events were parameterized for the evergreen *Pinus sylvestris.*

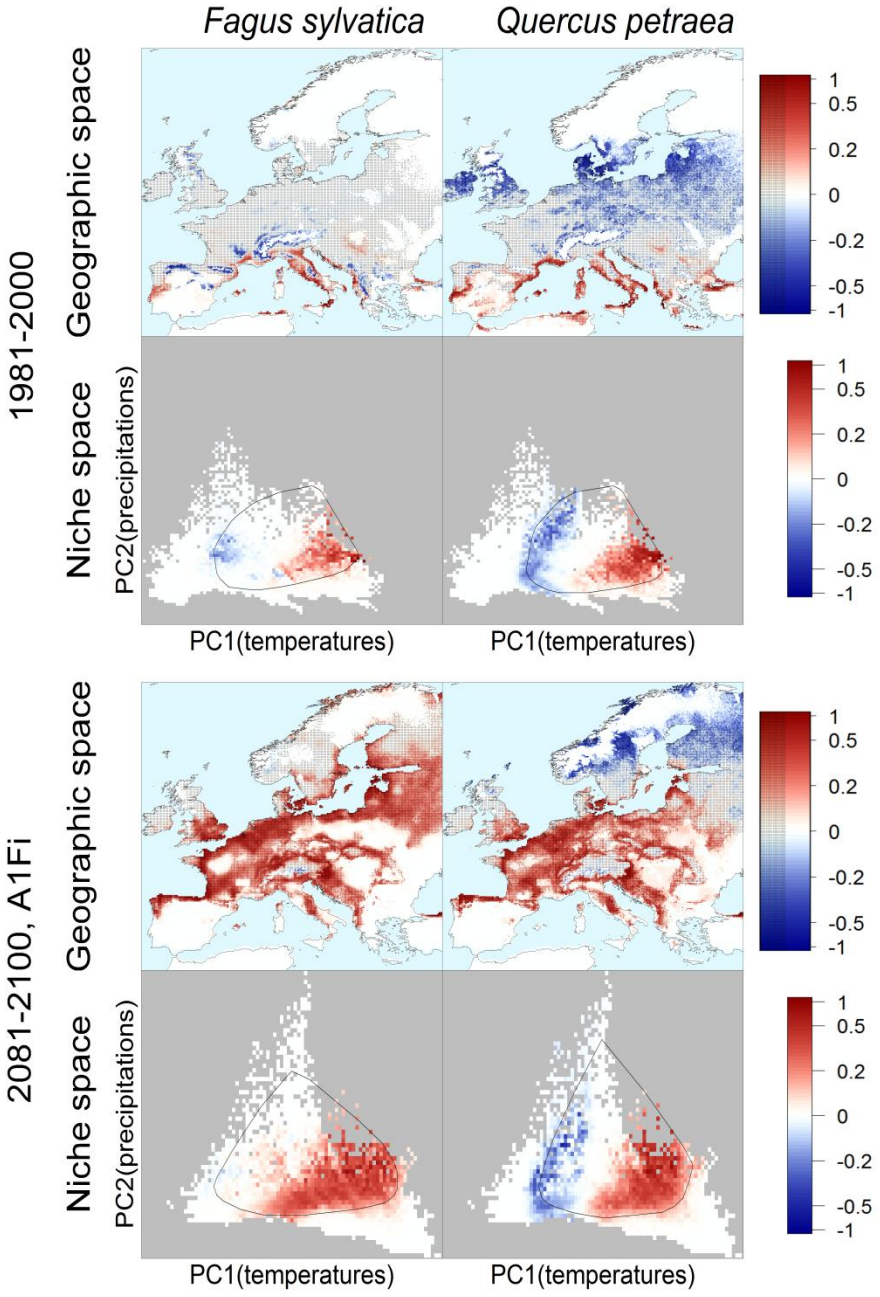

5. FIGURE S6

Figure S6. Projected fitness in the "plastic" treatment for the three species (columns) for 1981-2000, and 2081-2100, under the two greenhouse gas emission scenarios A1Fi and B2 (rows). Areas with projected fitness under 0.1 (where species are considered absent) appear in white.

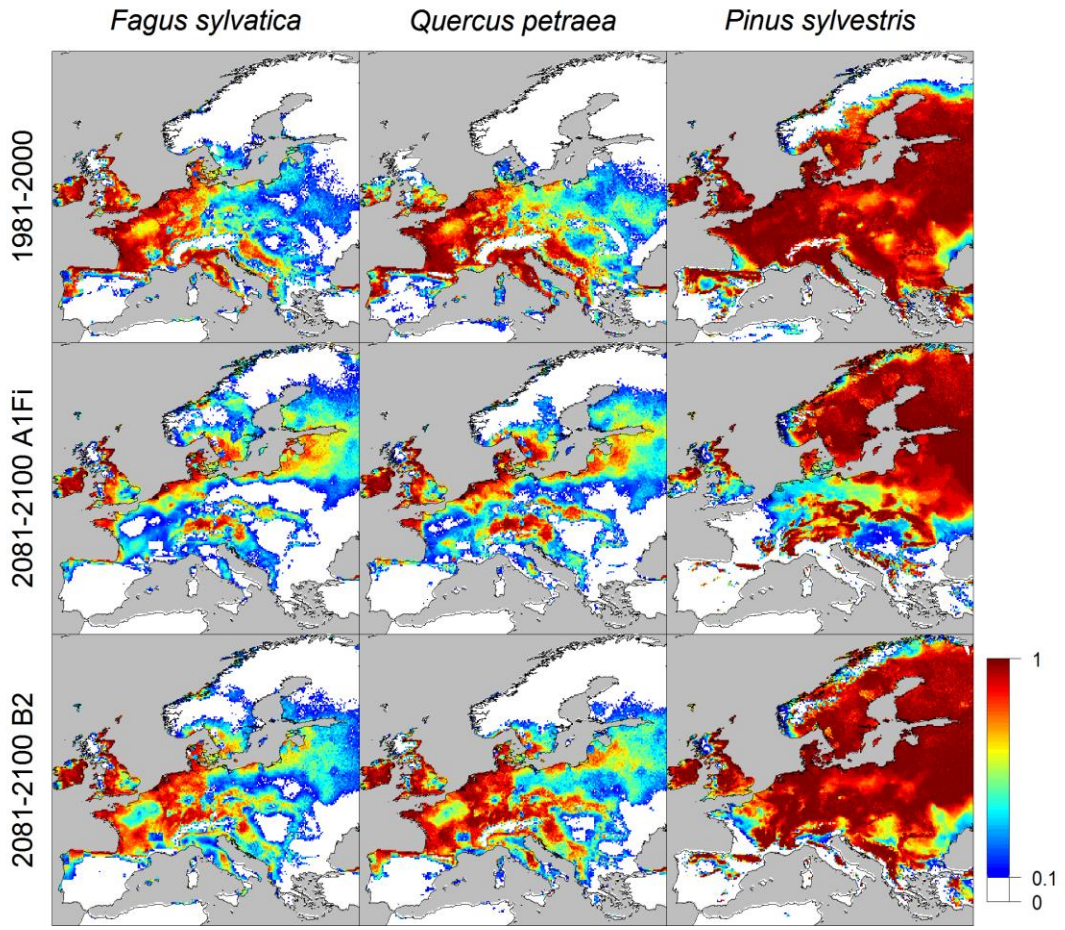

6. TABLE S3

Table S3. Changes in climatic niche size and geographic range size due to various components of phenotypic plasticity under historic conditions and climatic scenarios A1Fi and B2. In the geographic space, 10' pixels are weighted by their geographic area. Figures shown are relative to the "plastic" run (model 0). Model 0: Reference model with empirically fitted reaction norms. Models 1: Removing the effect of year-to-year fluctuations. Models 2: Removing the effect of spatial variation. Models 3: Removing the effect of trend variation.

Trait	Contribution of expressed part of plasticity		*Fagus sylvatica*			*Quercus petraea*			*Pinus sylvestris*		
			1981-2000	2081-2100 A1Fi	2081-2100 B2	1981-2000	2081-2100 A1Fi	2081-2100 B2	1981-2000	2081-2100 A1Fi	2081-2100 B2
			Niche change								
Spring events (models a)	Interannual	0-1a	1.8%	1.8%	0.8%	3.5%	3.1%	2.3%	3.0%	7.9%	3.6%
	Spatial	1a-2a	1.9%	8.3%	7.7%	-1.8%	-7.2%	-7.9%	-25.3%	-39.3%	-34.4%
	Trend	2a-3a	-	5.3%	3.4%	-	7.8%	5.0%	-	-1.4%	0.2%
	Total	0-3a or 0-2a	3.7%	15.4%	11.9%	1.7%	3.6%	-0.5%	-22.3%	-32.8%	-30.6%
Fall events (models b)	Interannual	0-1b	-0.6%	-1.6%	-1.1%	-0.4%	-1.4%	-0.3%			
	Spatial	1b-2b	4.8%	18.2%	15.5%	4.5%	6.7%	5.9%			
	Trend	2b-3b	-	15.3%	12.0%	-	10.6%	5.6%			
	Total	0-3b or 0-2b	4.2%	31.9%	26.4%	4.1%	15.9%	11.2%			
Both (models c)	Interannual	0-1c	1.1%	0.5%	-0.4%	2.6%	1.5%	1.7%			
	Spatial	1c-2c	9.7%	22.3%	22.2%	1.7%	3.6%	3.9%			
	Trend	2c-3c	-	12.5%	9.2%	-	12.7%	8.5%			
	Total	0-3c or 0-2c	10.8%	35.3%	31.1%	4.2%	17.8%	14.0%			
			Range change								
Spring events (models a)	Interannual	0-1a	2.0%	3.3%	1.9%	7.9%	5.5%	4.4%	3.4%	16.8%	5.0%
	Spatial	1a-2a	2.3%	14.9%	5.6%	-10.1%	1.3%	-3.4%	-19.3%	-59.7%	-31.4%
	Trend	2a-3a	-	9.0%	4.5%	-	13.3%	6.2%	-	-2.0%	0.0%
	Total	0-3a or 0-2a	4.3%	27.2%	12.0%	-2.2%	20.1%	7.1%	-15.9%	-45.0%	-26.5%
Fall events (models b)	Interannual	0-1b	0.0%	-2.2%	-0.5%	-0.5%	-0.8%	-0.8%			
	Spatial	1b-2b	1.8%	20.5%	9.1%	-1.5%	15.1%	3.5%			
	Trend	2b-3b	-	27.0%	14.7%	-	14.8%	4.9%			
	Total	0-3b or 0-2b	1.7%	45.3%	23.4%	-2.0%	29.1%	7.5%			
Both (models c)	Interannual	0-1c	2.0%	0.6%	1.3%	7.4%	4.3%	3.6%			
	Spatial	1c-2c	4.7%	27.4%	14.2%	-8.9%	17.4%	3.4%			
	Trend	2c-3c	-	27.2%	17.8%	-	18.0%	8.3%			
	Total	0-3c or 0-2c	6.7%	55.1%	33.3%	-1.5%	39.7%	15.3%			

7. FIGURE S7

Figure S7. As main text Fig. 2 but showing results for both scenarios. This figure shows the total effect of plasticity (treatment 0 – treatment 2c for the historical period; treatment 0 – treatment 3c for the two scenarios), in the geographic (top rows) and climatic (bottom rows) spaces.

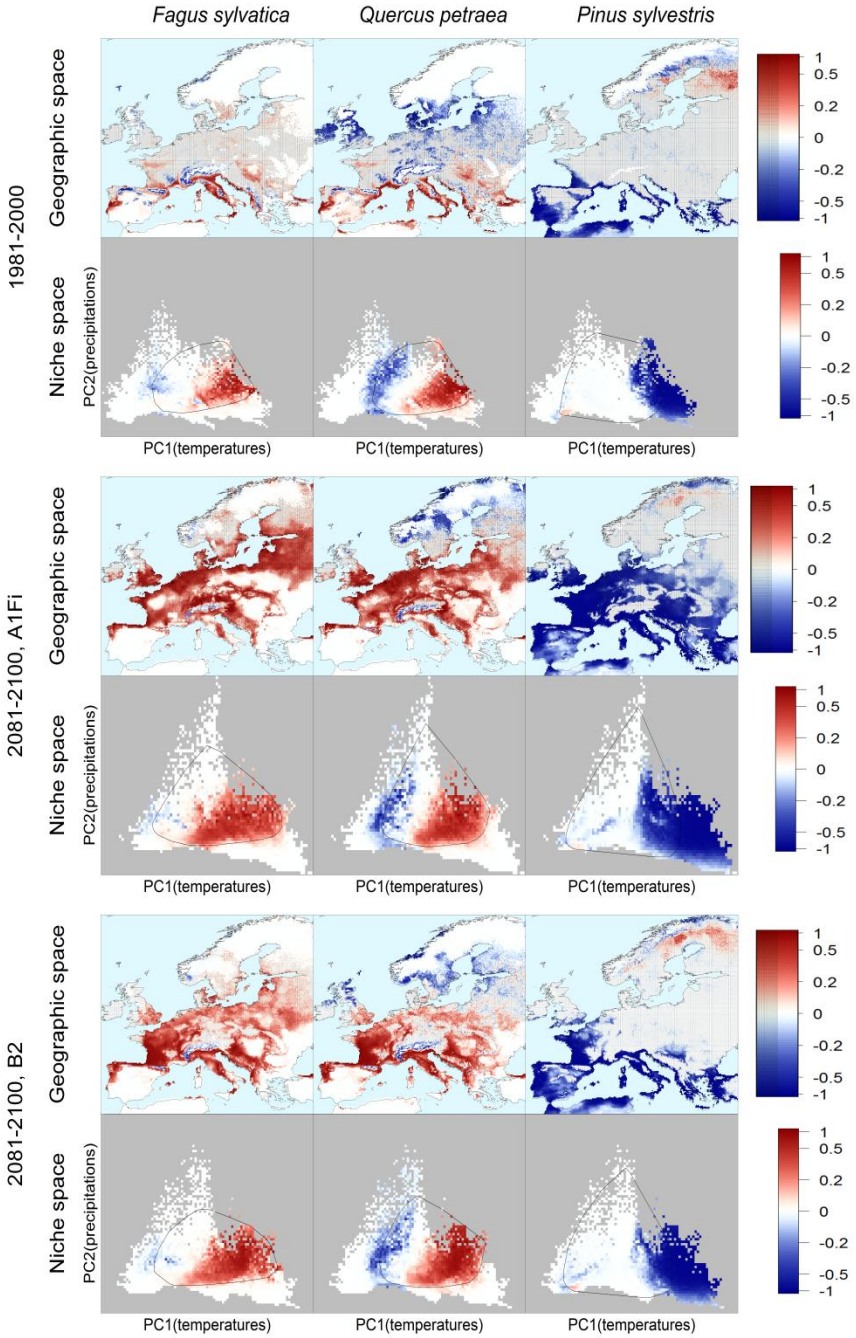

8. FIGURE S8

Figure S8. As main text Figure 3, but under scenario B2. Boxplot showing fitness gains (positive values) or losses (negative values) due to plasticity for the three species (columns), as a function of classes of fitness difference between 2081-2100 (scenario B2) and 1981-2000 (colonised, increased, decreased, gone extinct, absent). Top row: fitness contribution of interannual variation in trait means (treatment 0 minus treatment 1c). Middle row: fitness contribution of geographical variation in trait means (treatment 1c minus treatment 2c). Bottom row: fitness contribution of trend variation in trait means (treatment 2c minus treatment 3c). Stars indicate significant difference from zero at the 1% level, with star location relative to the median show the sign of the difference; and **m** denote *p*-values between 1% and 5%.

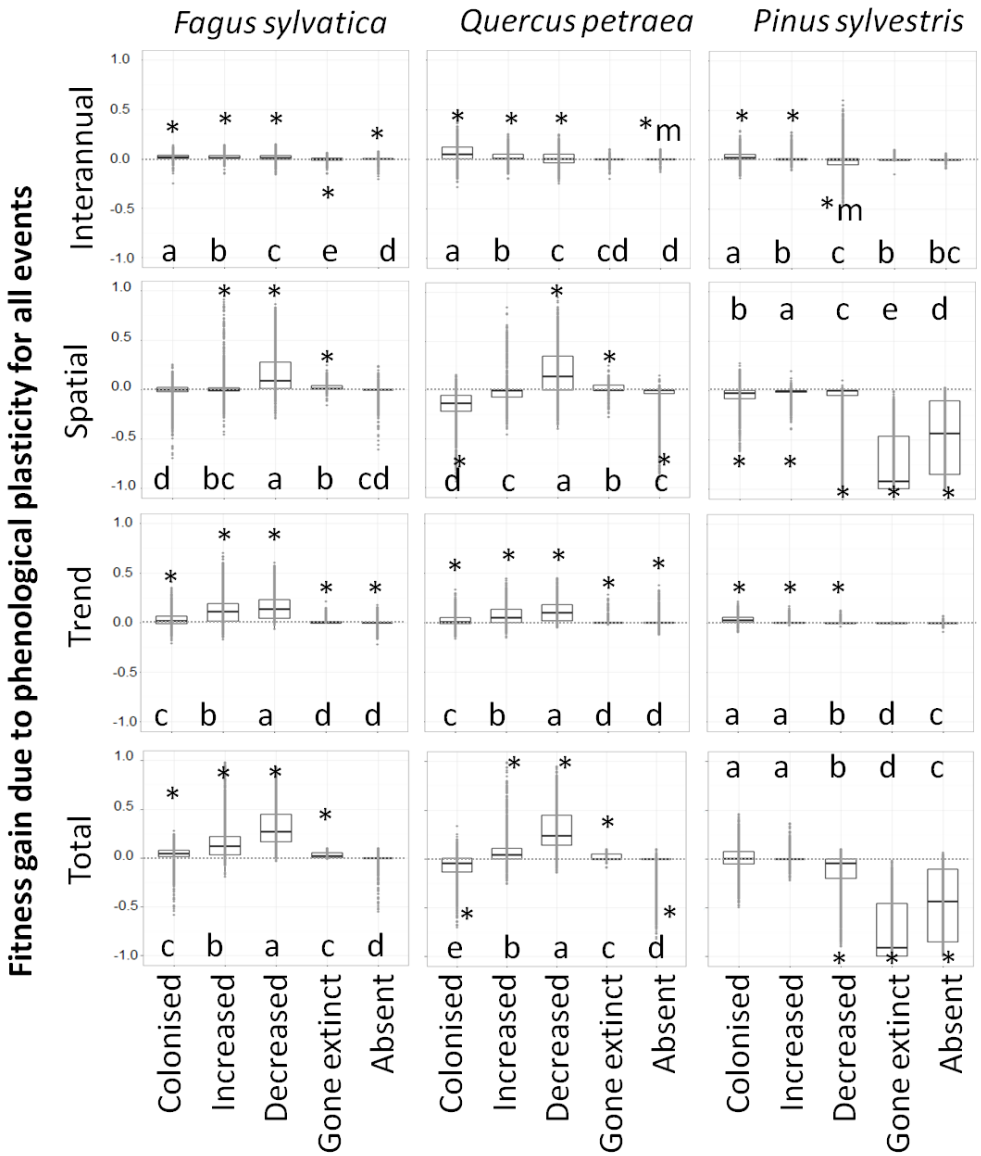

9. FIGURE S9

Figure S9. As main text Fig. 4 but showing results in the geographic space only. First and second rows refer to historical conditions. Top row: effect of the interannually expressed part of phenological plasticity (model 0 – model 1c); second row: effect of the spatially expressed part of phenological plasticity (model 1c – model 2c). Third to fifth rows refer to scenario A1Fi. Third row: effect of the interannually expressed part of phenological plasticity (model 0 – model 1c); fourth row: effect of the spatially expressed part of phenological plasticity (model 1c – model 2c); fifth row: effect of the part of plasticity expressed over changing climatic conditions (model 2c – model 3c).

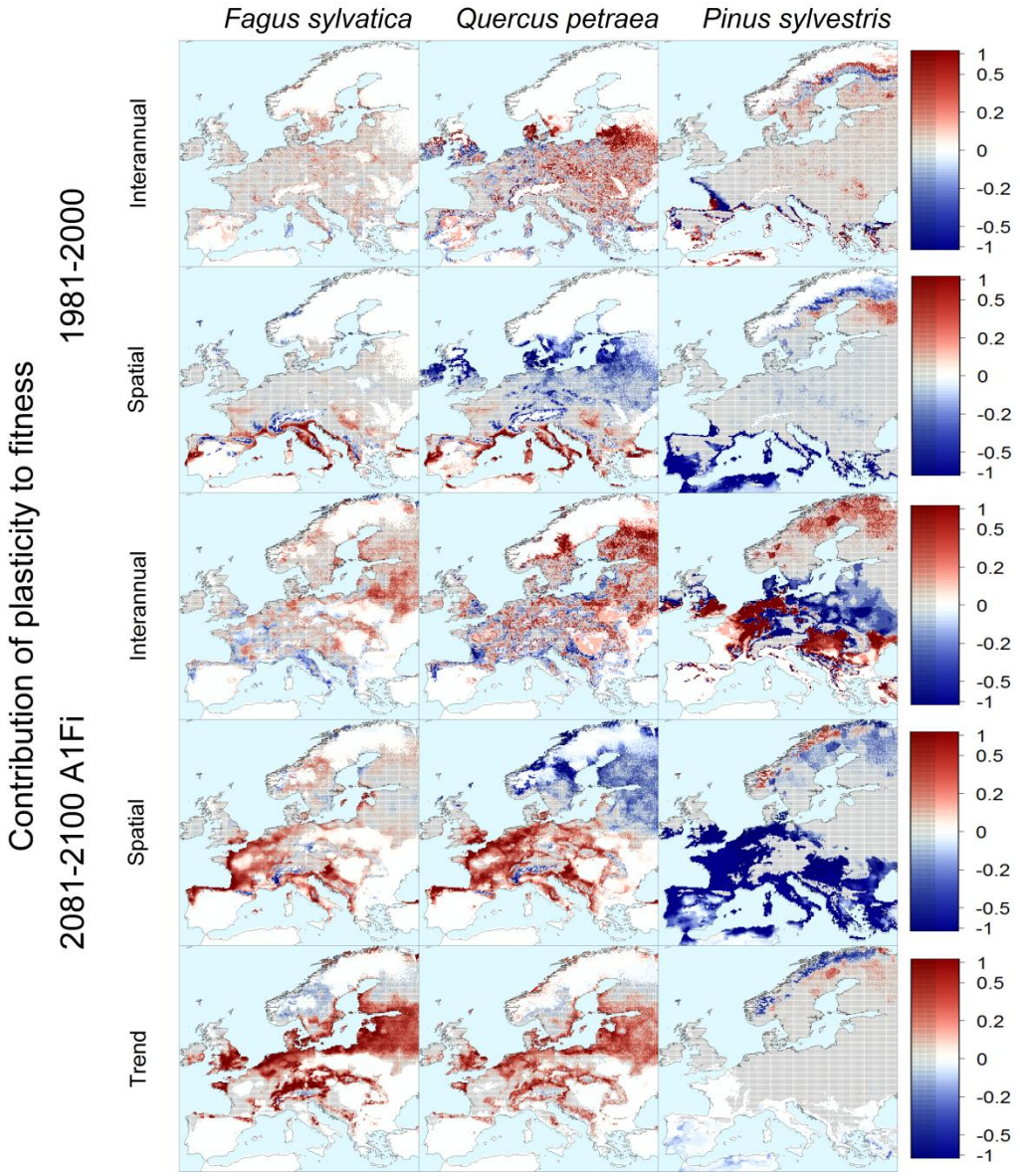

10. FIGURE S10

Figure S10. Leaf unfolding dates in the "plastic" treatment for the current period, and factors limiting fitness.
Top row: dates of leaf unfolding, as projected by the model PHENOFIT, for the current period (1981-2000). Black dots represent the regions where modeled fitness in model 0 exceeds 0.1.
Second row: density distribution (ordinates) of modelled leaf unfolding dates (abscissas) for pixels where the species is present (black line) and absent (grey line). This shows that predicted dates are mostly too late outside the range.
Bottom row: Factors limiting fitness in each pixel. The following method was applied sequentially:

- if mean yearly precipitations over 1981-2000 were outside the species' tolerance limits, the **hydric regime** was considered to limit survival; but if not:
- if the minimum temperature over 1981-2000 was below the species' tolerance threshold, **lethal frost** was considered to limit survival; but if not:
- if bud dormancy failed to break on 6 or more years over the 20-year period, **dormancy break** was considered as the limiting factor; but if not,
- if the mean LAI over the years when leaf unfolding occurred was below 0.5, this meant leaves had formed but had frozen; **leaf frost** was the limiting factor; but if not,.
- if the maturation index was low (on average below 0.5) for any other reason, **low maturation success** was the limiting factor; and,
- if none of the above applied, **fitness was not considered to be strongly limited.**

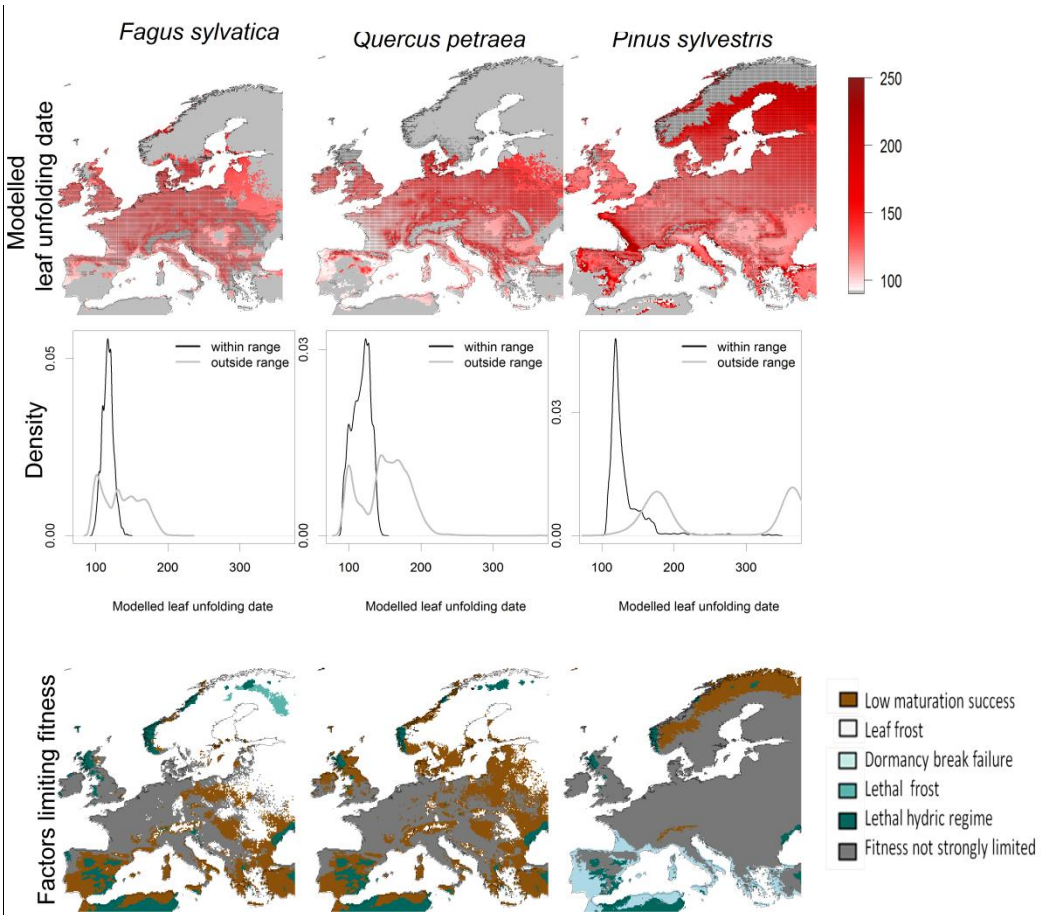

11. FIGURE S11

Figure S11. Predicted mean seed set of sessile oak (1950-2000) at a location in northeastern France (5°E, 49°N), for various imposed fixed dates of leaf unfolding and flowering. Maximal seed set is obtained for a wide range of dates; it decreases slowly from the optimum as the date of leaf unfolding advances due to frost damages; and it abruptly declines for late dates of leaf unfolding due to shortened growing season hampering fruit maturation. Fecundity curves in other locations have the same shape.

Under current conditions, marginal areas often correspond to locations with suboptimal phenology (resulting in low maturation success or increased frost damage; Fig. S9). The three circles represent leaf unfolding dates in three hypothetical locations respectively at the range center (grey), closer to the edge (blue, "inner margin") and just outside the range (red, "outer margin"), and arrows apart from the circles represent the interannual variability of the date. Within the range of all three species, leaf unfolding occurs over a wide range of dates (line 2 of Fig. S9), thus seed set is maximal over a wide window (plateau on the figure): within this range, interannual variation in leaf unfolding and flowering dates is almost neutral. Outside this range, seed set decreases rapidly. In marginal locations where bud burst date occurs either too early or too late, causing low maturation success or frost damage (Fig. S9), interannual variation in phenology can have two different outcomes. If the trait value is far away from the optimum, that is, towards the outer margin of the distribution (red dot and red pixels on Figs. 2, 4), variations around the trait mean on average result in increasing the seed set. If the trait value is not very far away from the optimum, resulting in intermediate seed set, variations around this mean are more likely to result in a reduction than in an increase of seed set (blue dot and blue pixels on Figs. 2, 4).

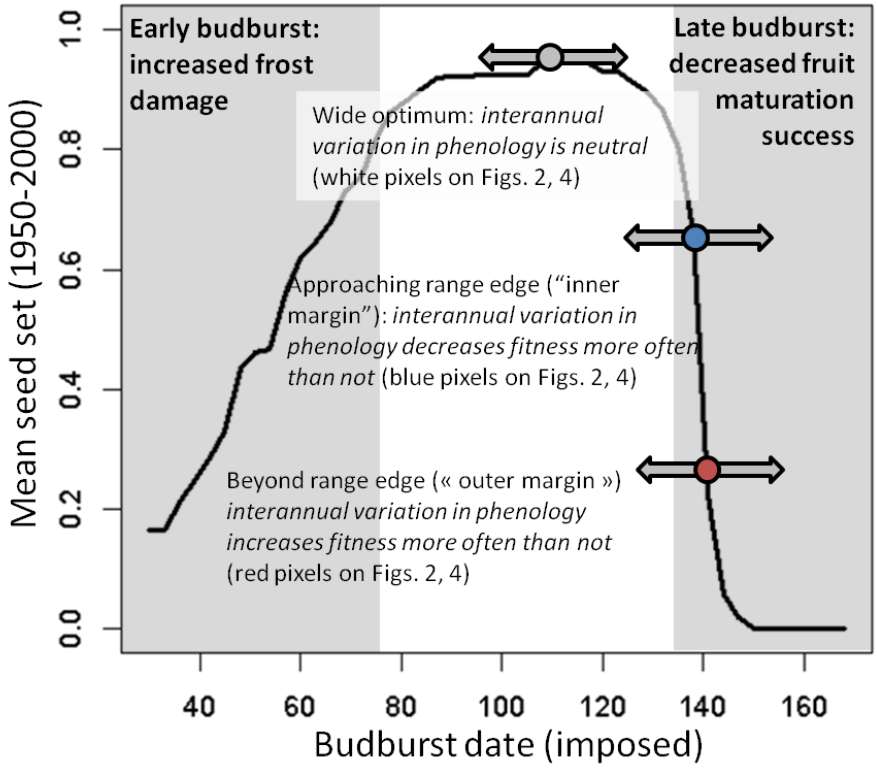

IV. REFERENCES

Bohn, U., Gollub, G., Hettwer, C., Neuhäuslová, Z., Raus, T., Schlüter, H., *et al.* (2004). Karte der natürlichen Vegetation Europas Map of the Natural Vegetation of Europe. Interaktive/Interactive CD-ROM - Erläuterungstext, Legende, Karten / Explanatory Text, Legend, Maps. Landwirtschaftsverlag, Münster.

Charrier, G. (2011). *Mécanismes et modélisation de l'acclimatation au gel des arbres - Application au noyer Juglans regia L. PhD thesis, Université d'Auvergne, France.*

Cheaib, A., Badeau, V., Boe, J., Chuine, I., Delire, C., Dufrêne, E., *et al.* (2012). Climate change impacts on tree ranges: model intercomparison facilitates understanding and quantification of uncertainty. *Ecol. Lett.*, 15, 533–44.

Chuine, I. (2000). A unified model for budburst of trees. *J. Theor. Biol.*, 207, 337–347.

Chuine, I. & Beaubien, E.G. (2001). Phenology is a major determinant of tree species range. *Ecol. Lett.*, 4, 500–510.

Chuine, I., Cour, P. & Rousseau, D.D. (1998). Fitting models predicting dates of flowering of temperate-zone trees using simulated annealing. *Plant, Cell Environ.*, 21, 455–466.

Chuine, I., Garcia de Cortazar Atauri, I., Kramer, K. & Hänninen, H. (2013). Plant development models. In: *Phenol. an Integr. Environ. Sci.* (ed. Schwartz, M.D.). Kluwer Academic Publishers, Dordrecht, The Netherlands.

Delpierre, N., Dufrêne, E., Soudani, K., Ulrich, E., Cecchini, S., Boé, J., *et al.* (2009). Modelling interannual and spatial variability of leaf senescence for three deciduous tree species in France. *Agric. For. Meteorol.*, 149, 938–948.

Duputié, A., Zimmermann, N.E. & Chuine, I. (2014). Where are the wild things? Why we need better data on species distribution. *Glob. Ecol. Biogeogr.*, 23, 457–467.

Gritti, E.S., Duputié, A., Massol, F. & Chuine, I. (2013). Estimating consensus and associated uncertainty between inherently different species distribution models. *Methods Ecol. Evol.*, 4, 442–452.

Jalas, J. & Suominen, J. (n.d.). *Atlas Florae Europaeae*. The Committee for Mapping the Flora of Europe and Societas Biologica Fennica Vanamo, Helsinki, Finland.

Kramer, K. (1994). A modelling analysis of the effects of climatic warming on the probability of spring frost damage to tree species in The Netherlands and Germany. *Plant, Cell Environ.*, 17, 367–377.

Lahti, T. & Lampinen, R. (1999). From dot maps to bitmaps: Atlas Florae Europaeae goes digital. *Acta Bot. Fenn.*, 162, 5–9.

Leinonen, I. (1996). A simulation model for the annual frost hardiness and freeze damage of Scots pine. *Ann. Bot.*, 78, 687–693.

Morin, X., Améglio, T., Ahas, R., Kurz-Besson, C., Lanta, V., Lebourgeois, F., *et al.* (2007). Variation in cold hardiness and carbohydrate concentration from dormancy induction to bud burst among provenances of three European oak species. *Tree Physiol.*, 27, 817–825.

Sakai, A. & Weiser, C.J. (1973). Freezing resistance of trees in North America with reference to tree regions. *Ecology*, 54, 118–126.

Sarvas, R. (1974). Investigations on the annual cycle of development of forest trees. II. Autumn dormancy and winter dormancy. *Commun. Instituti For. Fenn.*, 84, 1–101.

Swets, J. (1988). Measuring the accuracy of diagnostic systems. *Science*, 240, 1285–1293.

Vitasse, Y. (2009). *Déterminismes environnemental et génétique de la phénologie des arbres de climat tempéré. PhD thesis, Université Bordeaux 1, France.*

Wang, E. & Engel, T. (1998). Simulation of phenological development of wheat crops. *Agric. Syst.*, 58, 1–24.